

¹Ravi Kumar Goyal²Uma Shankar Modani

Design of circular slots loaded MIMO antenna with DGS at 28 GHz for 5G wireless services



Abstract: - In this paper, a MIMO microstrip patch antenna with four radiating elements is designed and analyzed at 28 GHz. This paper addresses the problem of mutual coupling without adding a decoupling network. The decoupling method increases the complexity and volume of MIMO antennas. The CST Microwave simulator is used to simulate the MIMO antenna. The simulation and measurement results are compared to analyze the antenna's performance. The parameters of the MIMO patch antenna, including return loss, VSWR, gain, beam width, and radiation pattern, are evaluated at a center frequency of 28 GHz. The overall dimensions of the MIMO antenna are $60 \times 42 \times 1.6 \text{ mm}^3$. An H-shaped slot is inserted in the middle of the ground plane to minimize mutual coupling among the radiating elements. The isolation amplitude between radiating elements is observed greater than 35 dB at 28 GHz frequency. A wide impedance bandwidth of 4 GHz (26.5 to 30.5) is achieved, by etching four small arcs into the patch's corners. In this work, two circular slots are inserted on the radiating element to widen the bandwidth further by adjusting the surface current on each radiating patch. At the center frequency of 28 GHz, the Envelope Correlation Coefficient (ECC) is observed to be 0.0001, with a diversity gain of 10 dB. The antenna has a maximum radiation efficiency of 75% and a peak gain of 7.62 dB. This antenna can be used for 5G wireless services.

Keywords: 5G; DG; ECC; MIMO; SISO

I. INTRODUCTION

The MIMO antenna system is a technology which provides higher capacity than a SISO (single input single output) system without increasing the bandwidth or transmits power level [1]. In MIMO system the space diversity approach is applied at the transmitter or receiver to improve the system reliability by reducing the effects of multipath fading [2]. The main challenge in multiple antenna design is to improve inter-element isolation of the antenna system [3]. Various studies have been reported in the literature [1-14] in this regard. In reference [1], the author has proposed two element MIMO antenna. However, the Isolation is only 20dB which is generally less. In reference [2], the author has designed dual band two elements MIMO antenna, wherein the achieved mutual coupling reduction is around 31 dB and gain are observed to be 5.7 dB. In reference [3], two ports MIMO antenna with dual band is proposed. However, the gain of the MIMO antenna is only 5.2 dB which is generally less for MIMO system. In reference [4] four elements MIMO antenna with decoupling line is presented. The isolation between antenna elements is 25 dB. However, decoupling techniques tends to increase the complexity of MIMO antennas and require more volume. In references [5] the design of four elements MIMO is presented. However, the isolation of the MIMO antenna is only 20 dB which is generally less for MIMO system antenna. Reference [6] proposed MIMO antenna of size of $20 \times 45 \text{ mm}^2$ with isolation of about 25 dB. In references [7] – [13], different MIMO antennas with different sizes are designed for 5G applications. In reference [14], the design of a MIMO antenna for an UWB system with a size of $60 \times 35 \text{ mm}^2$ is presented. The isolation is only 17 dB, which is generally less for MIMO systems.

In this paper, four-port MIMO antenna with circular slots loaded radiators is proposed without utilizing a decoupling network. In this design, an H-shape slot is inserted in the middle of ground plane to block the surface current transmission. The four radiators are placed orthogonally to reduce mutual coupling. In this proposed work, isolation greater than 35 dB, gain per element better than 7.62 dB, bandwidth of 4GHz is achieved. The novelty of the paper is the design of four radiating patches in an orthogonal configuration, thereby avoiding the usage of any decoupling structure and the circular slots on the radiating patch provide a wide bandwidth. The comparison work of recently reported paper with proposed work is listed in Table 2. The MIMO antenna parameters like ECC, isolation loss, peak gain are better than the literature structures.

¹*Corresponding author: Engineering College Ajmer

²Engineering College Ajmer

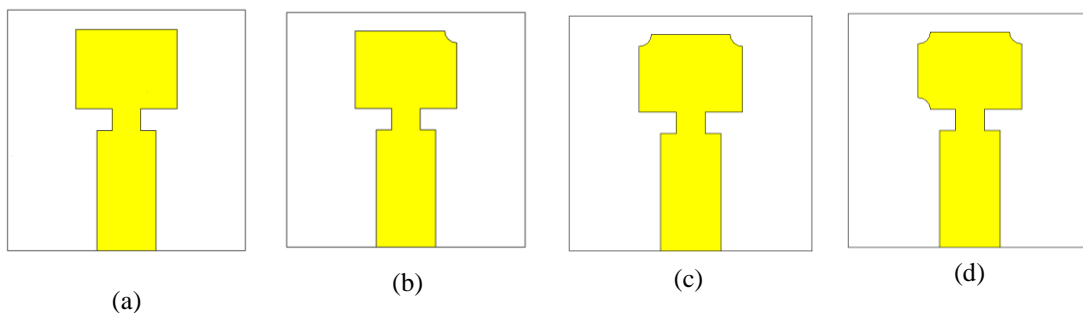
Copyright©JES2024on-line:journal.esrgroups.org

II. ANTENNA DESIGN

The step-by-step design evolutions are illustrated in Fig.1. In step 1 the rectangular patch with dimension of $6.5 \times 8.5 \text{ mm}^2$ is designed to resonate at 29 GHz frequency. At the second step, a semi-circle with a radius of 0.5 mm is inserted at the corner of the patch on the right side of the patch. Similarly, at steps 3, 4, and 5, semi-circles with a radius of 0.5 mm are inserted at the remaining corners of the patch to avoid abrupt changes at the corners of the radiator. At step 6, a circular slot of diameter 3 mm is inserted into a conductor plate to improve the bandwidth. At the final step 7, another circular slot of the same diameter is introduced to increase the electric length of the antenna and better match the impedance. These slots are placed and oriented in a manner to maximize the radiation output. The patch is fed by a 50Ω microstrip line with a quarter wavelength transformer line of the size of $1.8 \times 0.75 \text{ mm}^2$. The dimensions of micro strip line are $10 \times 5 \text{ mm}^2$. The dimensions of the ground plane are $60 \times 42 \text{ mm}^2$. It is further slightly modified in the ground plane by cutting an H-slot between the radiating patches to improve the isolation. The proposed antenna along with its layout dimensions is shown in Fig. 2. The designed antenna is fabricated over Roger (RT5880) substrate of thickness of 1.6 mm and dielectric constant of 2.2 with loss tangent 0.0009. The overall size of MIMO antenna structure is $60 \times 42 \times 1.6 \text{ mm}^3$. Each patch element is fed through 50Ω microstrip feed line. K-type connectors are used to supply the power to each port. The fabricated prototype of designed structure is shown in Fig. 3. The depicted antenna is analyzed on CST Microwave Studio. Table 1 shows the detailed dimensional parameters of the proposed MIMO antenna structure.

Table 1 Dimensional parameters of the proposed four-element MIMO antenna structure

S. No.	Parameters	Variables	Dimensions(mm)
1.	Patch and Quarter-wave transmission line	W_p	8.5
		L_p	6.5
		L_t	1.8
		W_1	0.75
2.	Substrate	W_s	42
		L_s	60
		h	1.6
3.	Ground	W_g	42
		L_g	60
4.	Feeding line	W_f	5
		L_f	10
5.	Inter-element spacing	S	9
		d	5
6.	Radius of circular slots	r	1.5
7.	Radius of semi-circles	r_1	0.5
8.	Dimensions of slot in ground plane	l	12
		w	10



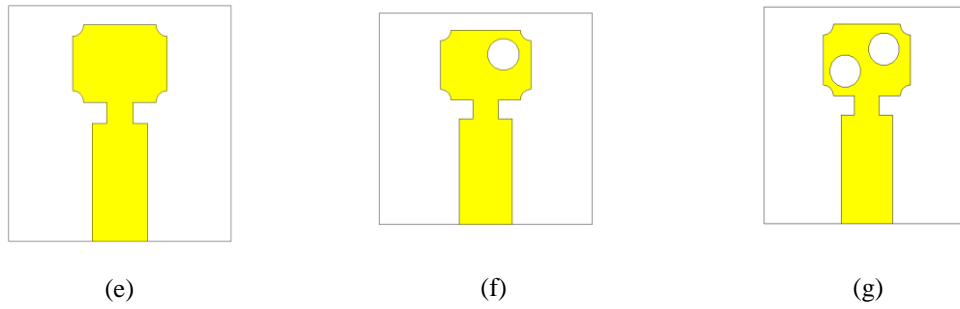


Figure 1 The evolution steps of the proposed antenna element (a) Antenna 1 (b) Antenna 2 (c) Antenna 3 (d) Antenna 4 (e) Antenna 5 (f) Antenna 6 (g) antenna7

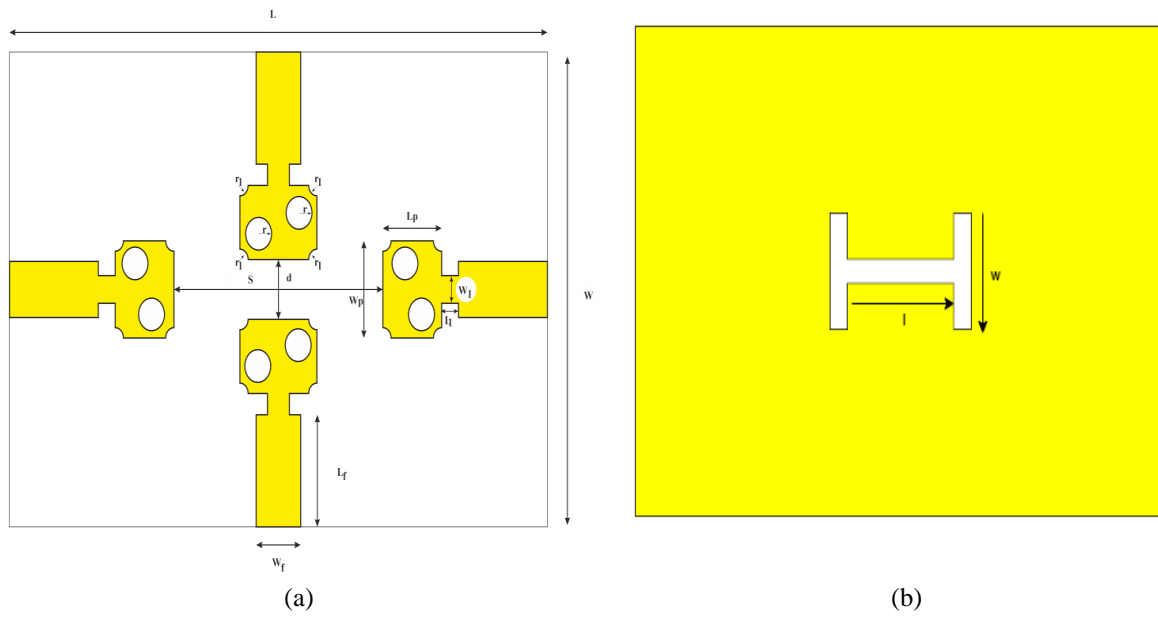


Figure. 2 Geometry of four-element MIMO antenna (a) Top view (b) Bottom view

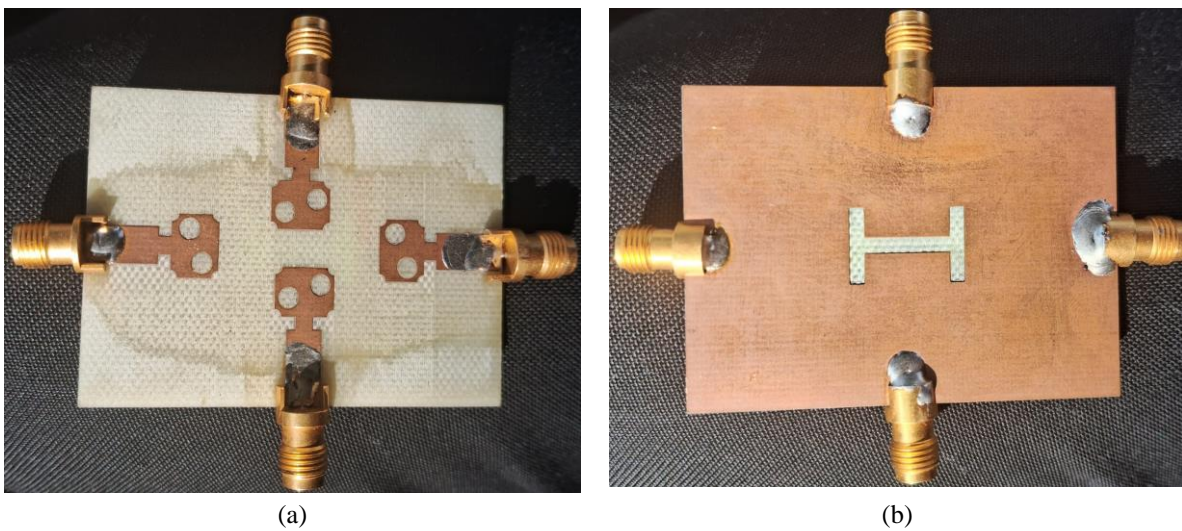


Figure 3 Fabricated prototype of four-element MIMO antenna (a) Top view (b) Bottom view

III. RESULT AND DISCUSSIONS

The simulations of the proposed MIMO antenna were carried out using the CST Microwave Studio simulation software. The parametric studies had been carried out to determine the optimal dimensions of the patch. There are several parameters that affect the operating frequency and bandwidth of the antenna. Fig. 4 shows the variation in length of a single radiator. The length of patch is varied from 6 mm to 6.6 mm, and the width is kept at 8.5 mm. It is inferred that increasing values of length shift the resonant frequency from higher to lower values. After performing the various studies of parametric analysis, the optimized values of length and width were finalized as 6.5 mm and 8.5 mm, respectively to retain the resonant frequency at 28 GHz for maximum bandwidth of 4 GHz. Fig. 5 demonstrates the simulated S_{11} -parameter curves as a function of frequency of antenna with and without circular slot. As shown in Fig. 5, cutting the circular slot at the patch can alter the operating frequency and bandwidth of the antenna. Fig. 6 illustrates the distribution of surface current density of the proposed MIMO antenna at 28 GHz. It is shown in Fig. 6 that the distribution of surface current is maximum at the surface of the one patch element, while the other patch elements have a lower current density on their surface when one port is excited and the other ports are terminated by 50Ω impedance. Isolation among the patch elements is improved by the insertion of an H-shaped slot in the middle of the ground, which serves as a barrier to the surface current. The S-parameters of the proposed antenna are measured using Agilent PNA network analyzer. The simulated and measured S_{11} -parameter curves as a function of MIMO antenna frequency are shown in Fig. 7. It is clear from Fig. 7 that there is a minimum return loss value of -50 for the simulated results and a minimum return loss of -25 dB for the measured results at port 1. Fig. 8 compares the simulated and measured S_{22} -parameters for the MIMO antenna at port 2. It is observed from Fig. 8 that the minimum return loss of -35 dB for simulated results and -25dB for measured results at port 2. The simulated and measured isolation loss plots the between port 1 and port 2 are also shown in Fig. 9. As shown in Fig. 9 the port-to-port isolation is less than -30 dB for simulation and measurement. The VSWR plot of the proposed MIMO antenna at port 1 is shown in Fig. 10. The impedance bandwidth for the case $VSWR < 2$ is observed as 4 GHz (26.5–30.5 GHz), which indicates a good impedance match of the patch antenna with 50Ω transmission line at the 28 GHz. The peak gain is observed at 7.62 dB at the 28 GHz spectrum, as shown in Fig. 11. The simulated Envelope Correlation Coefficient (ECC) of MIMO Antenna is observed at 0.0001 as shown in Fig.12. The diversity gain is observed at a 10 dB of the MIMO antenna in the diversity gain trace, as shown in Fig. 13. The radiations pattern of the MIMO antenna in the E-plane and H-plane at the 28 GHz are shown in Fig. 14. It is observed that when port 1 is excited and other ports are terminated by characteristic impedance (50Ω), the maximum radiations are in bore sight direction as depicted in Fig. 14. The beam width of the MIMO antenna is found as 38 degrees in E-plane and 60 degrees in H-plane as shown in Fig. 14 (a) and 14 (b) respectively.

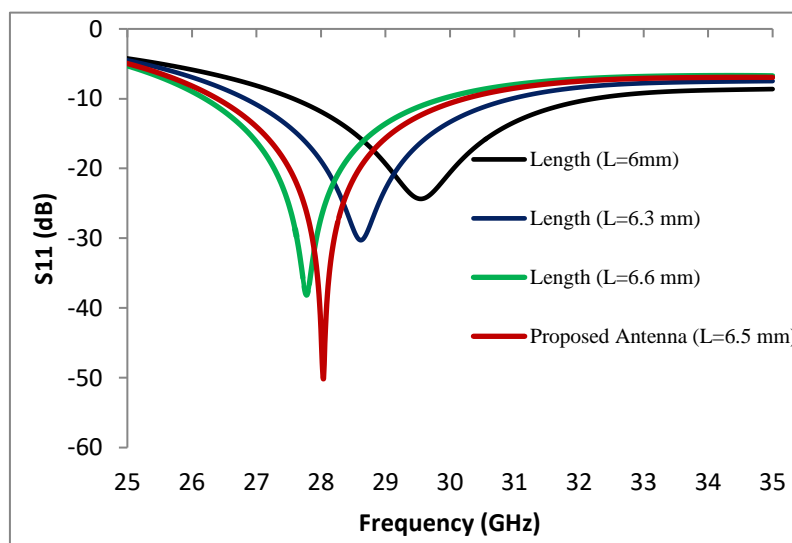


Figure. 4 Parametric study with length of a single radiator

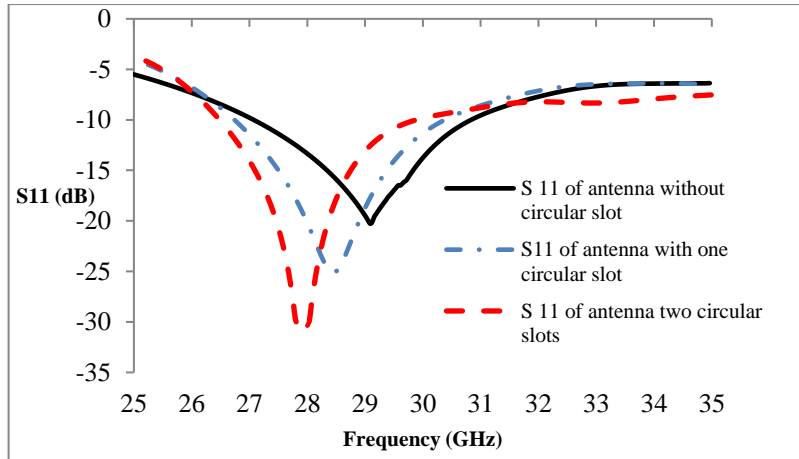


Figure. 5 Parametric study with antenna evolutions

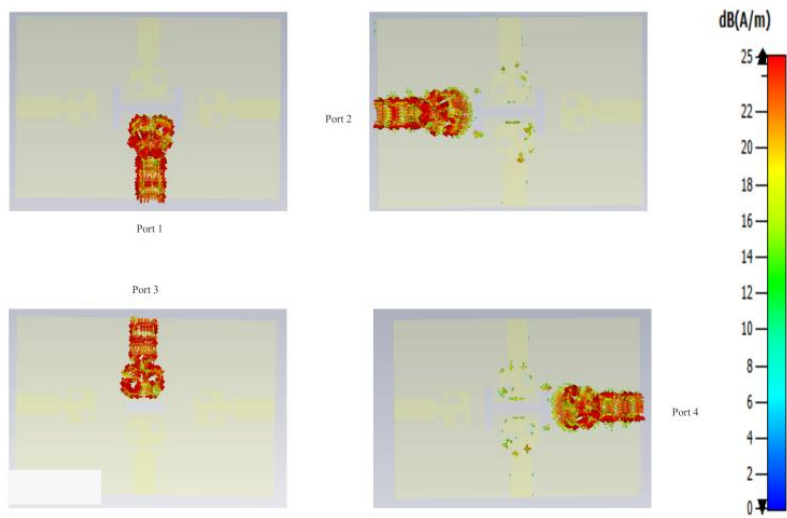


Figure. 6 Current distributions of the MIMO antenna (a) Port 1(b) Port 2 (c) Port 3 and, (d) Port 4 are excited sequentially

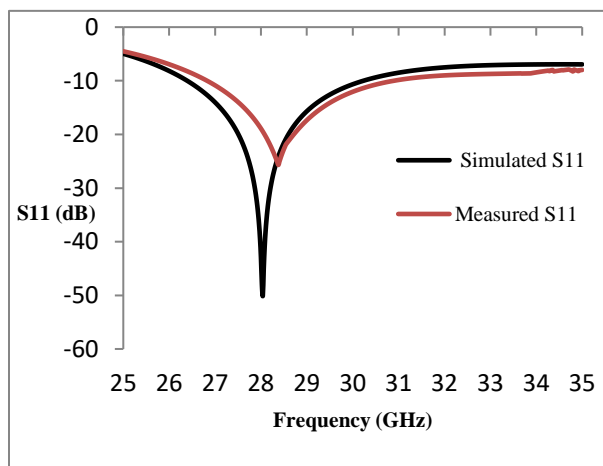


Fig. 7 The S_{11} plots of the MIMO antenna

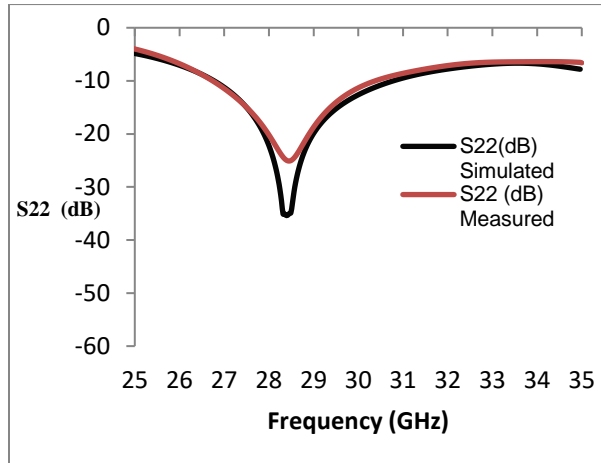


Figure. 8 The S22 plots of the MIMO antenna.

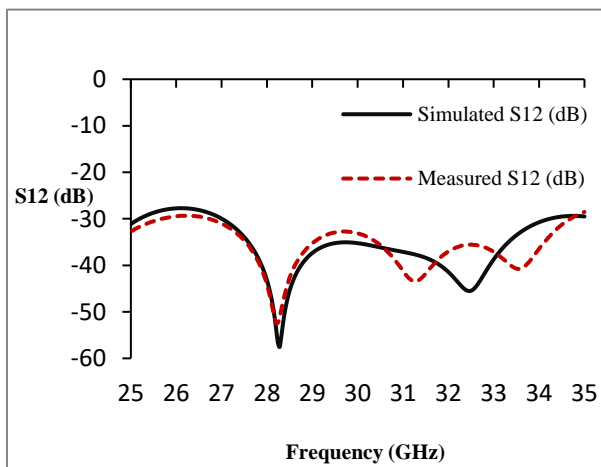


Figure. 9 Isolation loss plots of the MIMO antenna

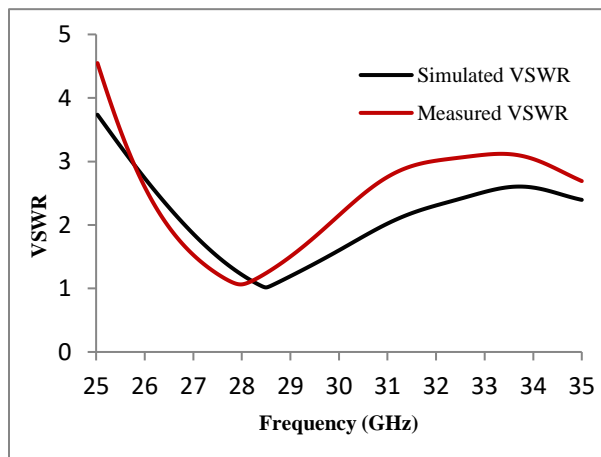


Figure. 10 The VSWR plot of the MIMO antenna at port 1

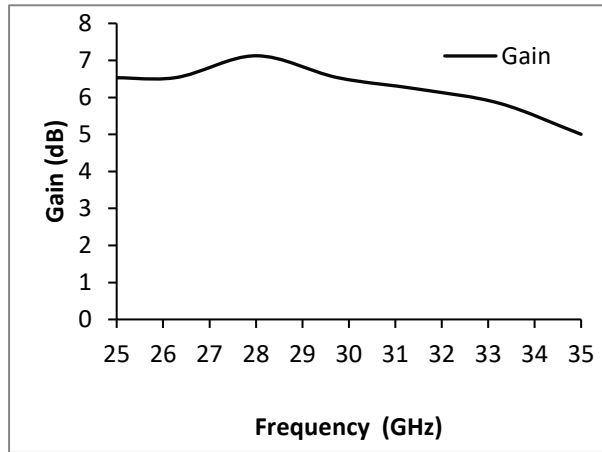


Figure 11 The gain plot of the MIMO antenna

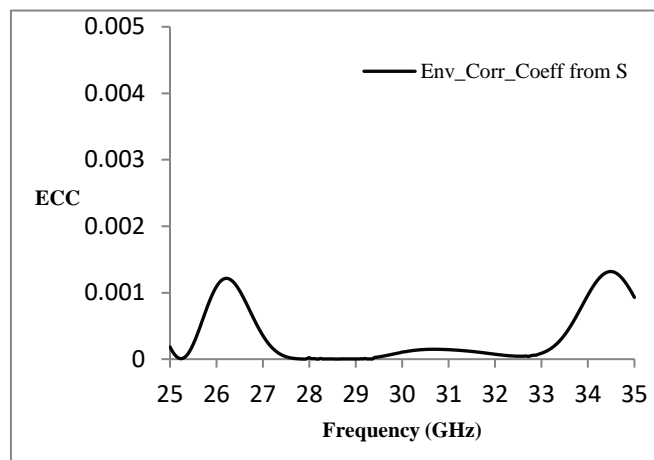


Figure12 The ECC plot of MIMO antenna

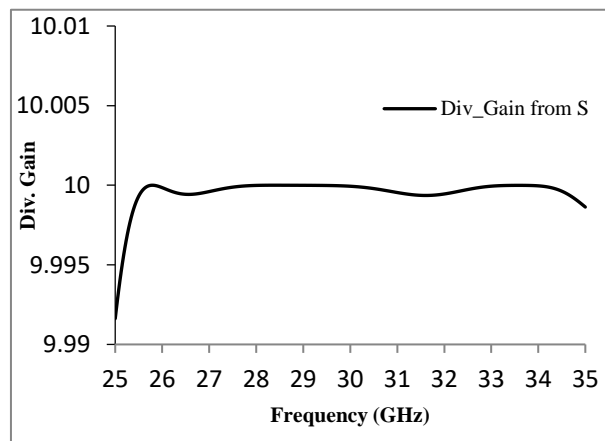


Figure.13 Diversity gain plot

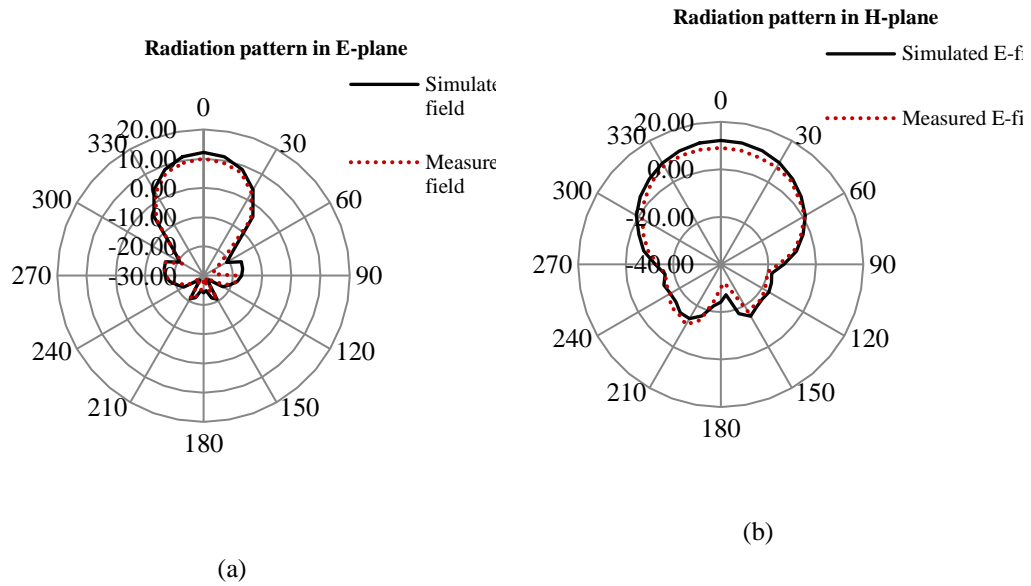


Figure 14 The radiation patterns of MIMO antenna when port 1 is excited (a) E-plane and (b) H-plane

Table 2 Comparisons among proposed work and recent published papers

Ref.	Overall Size (mm ³)	Resonance Frequency (GHz)	Ports	S12/S21 (dB)	Bandwidth (GHz)	Peak Gain (dBi)	ECC(dB)
[2]	30 × 15 × 0.203	28/38	2	-31	25.5–30.5	5.7	0.0002
[3]	27.65 × 12 × 0.2	28/38	2	-30	26–30	5.2	0.0001
[4]	13.75 × 13.75 × 0.78	35	4	-25	24–39.6	4	0.02
[5]	13.16 × 13.5 × 0.8	28	4	-20	26.3–29.3	6.34	NS
[6]	20 × 45 × 1.6	5.5	2/4	-25	4.71–6.62	NS	0.05
[7]	109 × 88.5 × 1.6	5.8	2	-25	5.5–6.1	8	0.02
[8]	42.8 × 34.4 × 1.6	5.8	4	-30	5.5–6.4	5.2	0.001
[9]	19 × 30 × 0.8	UWB	2	-18	3.1–10.6	2.91	0.13
[10]	55 × 55 × 1.6	5.8	4	-32	5.6–6.4	5.3	0.0001
[11]	23 × 40 × 1.6	UWB	2	-17	2–11	6.2	<0.2
[12]	55 × 110 × 0.508	28/38	2	-29	27.5–28.6	7.18	0.0001
[13]	40 × 40 × 1.6	7.5	4	-26	7.28–7.71	5.18	0.02
Proposed work	60 × 42 × 1.6	28	4	-50	26.5–30.5	7.62	0.0001

IV. CONCLUSION

This paper describes a topology of four-element MIMO antenna design in which antenna elements are positioned orthogonally and an H-slot is inserted in the middle of the ground plane in order to ensure excellent port isolation. The interspacing between the patch is kept 9 mm which is larger than the patch width to reduce the mutual coupling between MIMO antenna elements. By etching small arcs into the patch's corners, it improves the impedance bandwidth of 4 GHz (26.5–30.5) with a resonant frequency of 28 GHz. In this work, two circular slots are inserted on the radiating element to widen the bandwidth. The peak gain of 7.62 dB has been achieved at the 28 GHz frequency. At the centre frequency of 28 GHz, The Envelope Correlation Coefficient (ECC) is observed to be 0.0001; with diversity gain of 10 dB. The measured radiation pattern is matched largely with the simulated radiation pattern.

ACKNOWLEDGMENT

R. K. and U. S. Modani, thanks to Professor K. K. Sharma of MNIT Jaipur for providing his guidance and support for research work.

REFERENCES

- [1] R. K. Goyal, "The design of two-element MIMO antenna system with polarized diversity at 28 GHz for 5G application," TechRxiv Preprint <https://doi.org/10.36227/techrxiv.21137215>, April, 2023.
- [2] W.A.E. Ali, A.A. Ibrahim and A.E. Ahmed, "Dual-Band millimeter wave 2×2 MIMO slot antenna with low mutual coupling for 5G Networks," *Wireless Pers. Communication*, vol. 129, pp. 2959-2976, March, 2023.
- [3] A. R. Sabek, W.A.E. Ali and A.A. Ibrahim, "Two-Element MIMO antenna with dual band (28/38 GHz) for 5G wireless communications," *Journal of Infrared, Milli and Terahz Waves*, vol. 43, pp. 335-348, May, 2022.
- [4] I. Rosaline, A. Kumar, P. Upadhyay and A. H. Murshed, "Four-element MIMO antenna system with decoupling lines for high-speed 5G wireless data communication," *International Journal of Antenna and Propagation*, vol. 2022, Article ID 9078929, pp. 1-13, 2022.
- [5] R. K. Goyal, U. S. Modani, "The four-element MIMO Antenna Design with low mutual coupling at 28 GHz for 5G Networks," *International Journal of Engineering & Advanced Technology (IJEAT)*, vol. 11, Issue 04, ISSN 2249-8958, April, 2022.
- [6] A. W. M. Saadh, P. Ramaswamy, T. Ali, "A CPW fed two and four element antenna with reduced mutual coupling between the antenna elements for wireless applications," *Applied Physics A*, vol. 88, pp. 1-18, 2021.
- [7] W. Shen, S. Pan, G. Li, Y. Feng, J. Li, P. Xiao, "Pattern diversity and defected ground structure for decoupling planar Yagi MIMO antenna," *AEU-International Journal of Electronics and Communications*, vol. 142, Article ID 153980, 2021.
- [8] K. Malaisamy, M. Santhi, and S. Robinson, "Design and analysis of 4×4 MIMO antenna with DGS for WLAN applications," *International Journal of Microwave and Wireless Technologies*, vol. 13, issue 09, pp. 979-985, 2021.
- [9] A. Kumar, A. Q. Ansari, B. K. Kanaujia, J. Kishor, and S. Kumar, "An ultra-compact two-port UWB-MIMO antenna with dual band-notched characteristics," *AEU-International Journal of Electronics and Communications*, vol. 114, 152997, 2020.
- [10] F. Andrade, Erik & Pérez, Ángel & Gomez Villanueva, Ricardo & Jardon-Aguilar, Hildeberto, "Characteristic mode analysis applied to reduce the mutual coupling of a four-element patch MIMO antenna using a defected ground structure," *IET Microwaves, Antennas & Propagation*, vol. 14, DOI: 10.1049/iet-map.2019.0570, 2020.
- [11] E. Thakur, N. Jaglan, S. D. Gupta, B. K. Kanaujia, "A compact notched UWB MIMO antenna with enhanced performance," *Progress In Electromagnetic Research Letter*, vol. 91, pp. 39-53, Doi:10.2528/PIERC18120202, 2019.
- [12] H. M. Marzouk, M. I. Ahmed, and A. H. Shaalan, "Novel Dual-Band 28/38 GHz MIMO Antennas for 5G Mobile Applications," *Progress In Electromagnetic Research C*, vol. 93, pp. 103-117, 2019.

- [13] A. Dkiouak, A Zakriti, M. El Ouahabi, N.A.Touhami, A. Mchbal, “ Design of a four-element MIMO antenna with low mutual coupling in a small size for satellite applications,” *Progress In Electromagnetic Research*, vol.85, pp. 95-104, 2019.